

Property-Based Optimization of Hydroxamate-Based γ -Lactam HDAC Inhibitors to Improve Their Metabolic Stability and Pharmacokinetic ProfilesEunhyun Choi,^{†,‡,∇} Chulho Lee,^{‡,∇} Misun Cho,[‡] Jeong Jea Seo,[‡] Jee Sun Yang,[‡] Soo Jin Oh,[§] Kiho Lee,^{||} Song-Kyu Park,^{||} Hwan Mook Kim,[⊥] Ho Jeong Kwon,[‡] and Gyoonee Han^{*,‡,‡,‡}[†]Severance Integrative Research Institute for Cerebral & Cardiovascular Disease, Yonsei University Health System, 250 Seongsanno, Seodaemun-Gu, Seoul 120-752, Republic of Korea[‡]Translational Research Center for Protein Function Control, Department of Biotechnology, Yonsei University, Seodaemun-gu, Seoul 120-749, Republic of Korea[§]Bioevaluation Center, Korea Research Institute of Bioscience and Biotechnology, Yangcheong, Ochang, Cheongwon, Chungbuk 363-883, Republic of Korea^{||}College of Pharmacy, Korea University, Yeongi, Chungnam 339-700, Republic of Korea[⊥]College of Pharmacy, Gachon University of Medicine and Science, Incheon 406-799, Republic of Korea[#]Department of Biomedical Sciences (WCU Program), Yonsei University, Seodaemun-gu, Seoul 120-749, Republic of Korea

S Supporting Information

ABSTRACT: Hydroxamate-based HDAC inhibitors have promising anticancer activities but metabolic instability and poor pharmacokinetics leading to poor in vivo results. QSAR and PK studies of HDAC inhibitors showed that a γ -lactam core and a modified cap group, including halo, alkyl, and alkoxy groups with various carbon chain linkers, improved HDAC inhibition and metabolic stability. The biological properties of the γ -lactam HDAC inhibitors were evaluated; the compound designated **8f** had potent anticancer activity and high oral bioavailability.

INTRODUCTION

Histone deacetylases (HDACs) and histone acetyltransferases (HATs) are involved in chromatin remodeling and transcription.¹ HATs activate transcription by releasing chromatin from histones, whereas HDACs lead to compaction of chromatin structures and suppression of gene expression.² Silencing of tumor suppressor genes, such as p21 and p53, represses apoptosis.^{3,4} HDACs are known to be related to tumorigenesis and cell differentiation by virtue of their gene silencing ability. Thus, HDAC inhibitors are considered intriguing anticancer agents.^{5,6} Hydroxamate-based HDAC inhibitors are well-known for their potent anticancer activity. The hydroxamate group, a controversial warhead, is often introduced as a potent zinc chelator for strong binding with metal in the active site of enzymes.⁷ Nevertheless, only suberoylanilide hydroxamic acid (SAHA, Zolinza, Vorinostat)⁸ (1) has been approved by the U.S. Food and Drug Administration. Other hydroxamate-based HDAC inhibitors including trichostatin A (TSA)⁹ (2) (Figure 1) have been developed but remain in clinical trials because of poor metabolic stability and pharmacokinetic (PK) profiles. Hydroxamate is easily metabolized through hydrolysis and glucuronidation by liver microsomes, but it results in PK problems.¹⁰ It is reported that SAHA has a short half-life of about 21–58 min when administered intravenously.¹¹ Despite these metabolic instabilities, hydroxamate-based HDAC inhibitors are still a promising anticancer candidate. We searched for

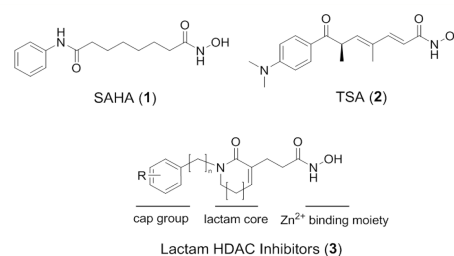


Figure 1. Chemical structures of hydroxamate-based HDAC inhibitors.

hydroxamate-based HDAC inhibitors with improved PK profiles using the property optimization process.

We designed and synthesized novel lactam-based HDAC inhibitors (3) composed of a cap group, lactam core, and hydroxamic acid.^{3–5,12–17} These analogues had good HDAC enzyme inhibitory and tumor growth inhibitory activities both in vitro and in vivo. Quantitative structure–activity relationship (QSAR) and docking studies demonstrated that the active site of the HDAC enzyme is a narrow pocket; a zinc ion in the interior active pocket interacts with the hydroxamic acid. The entrance of the active site is important in the hydrophobic interaction.¹⁸ PK studies and metabolic stability studies of δ -lactam-based HDAC inhibitors have shown that these

Received: July 3, 2012

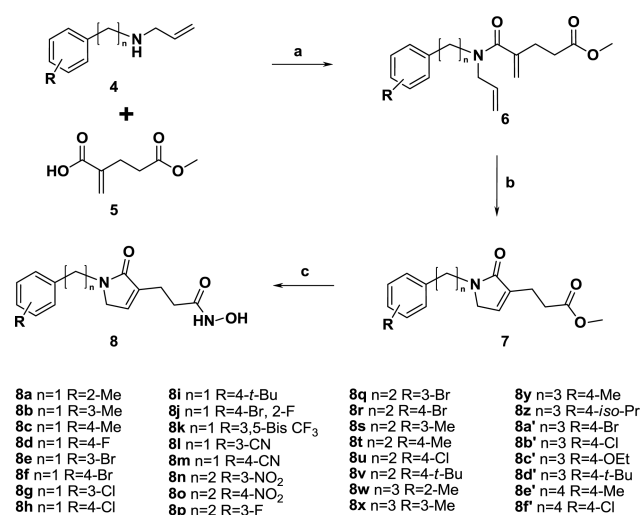
Published: November 19, 2012

analogues are metabolically unstable.^{4,14} Hydroxamic acid, a good zinc chelator, is easily hydrolyzed, and the hydrophobic cap group can be oxidized by liver microsomes. These reactions result in poor metabolic stability and eventually lead to poor PK profiles of the δ -lactam-based HDAC inhibitors. Our previous studies indicated that lipophilicity plays an important role in HDAC inhibition as well as PK profile. On the basis of these results, we changed the δ -lactam core to a γ -lactam core to reduce the core size and lipophilicity, and various substituents were introduced on the cap group to increase the metabolic stability by blocking the NIH shift.

RESULTS AND DISCUSSION

The synthetic process for producing γ -lactam analogues is shown in Scheme 1. EDC-mediated coupling with monoacid

Scheme 1. Synthesis of γ -Lactam-Based HDAC Inhibitors^a



^aReagents: (a) EDC, DMAP, CH₂Cl₂; (b) Grubbs' catalyst (2nd generation), CH₂Cl₂, reflux; (c) KOH₂ (1.7 M in MeOH), MeOH, 0 °C.

(5) with secondary amines (4), which were synthesized by *N*-alkylation or reductive amination, produced amides (6) with good yields. Metathesis reaction of amides with 2–3 mol % of Grubbs' catalyst (2nd generation) produced the γ -lactam rings (7) in high yields. Hydroxamic acid analogues (8) were obtained by reacting the esters of the γ -lactam with KOH₂ in MeOH at low temperature. The synthesized γ -lactam-based analogues contained one to four carbons between the cap group and γ -lactam core. Halo, alkyl, and alkoxy moieties were introduced as the cap groups in the ortho, meta, and para positions, respectively.

HDACs are classified into 11 isoforms. Among them, four isoforms have their X-ray structures in the Protein Data Bank (PDB): HDAC-2 (3MAX¹⁹), HDAC-3 (4A69), HDAC-7 (3C0Z), and HDAC-8 (1T69). These enzymes commonly have a narrow pocket and zinc ion in their active site. HDAC active sites are conserved structures, but they have slightly different shapes depending on the isoform. For example, the active site of HDAC-3 is shallower than that of the other isoforms and HDAC-2 has more room below the zinc. We performed docking simulations with human HDAC-2 using the Discovery Studio program.²⁰ On the basis of our previous study, the γ -lactam-based HDAC inhibitors had the most

selective inhibition against HDAC-6 of the HDAC isoforms;¹² however, the crystal structure of HDAC-6 is not yet available. Thus, human HDAC-2, the second most potent isoform, was used for the docking study. **8d**, **8f**, and **8i** with 4-fluoro, 4-bromo, and 4-*t*-butyl on the cap group, respectively, were used for the docking studies. The results show that γ -lactam-based HDAC inhibitors have a similar binding mode and orientation as SAHA in the active site. The hydroxamic acid chelated with the zinc ion and formed hydrogen bonds with His 145 and His 146. The γ -lactam core is located in the hydrophobic narrow pocket, stabilized by the π - π interaction between Phe 155 and Phe 210 (Figure 2).

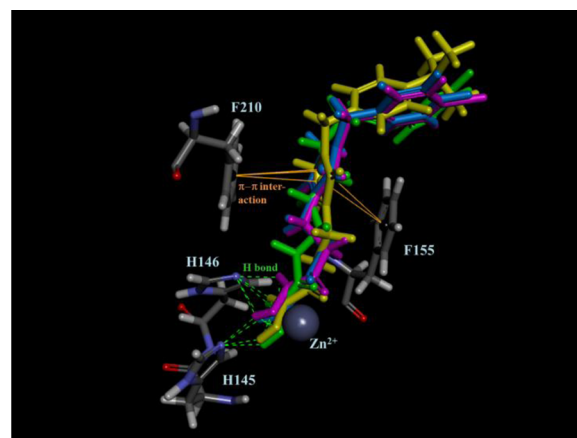


Figure 2. Docking simulation of **8d** (sky blue), **8f** (pink), **8i** (yellow), and SAHA (green) in human HDAC-2 active site (PDB 3MAX).

The potency of the synthesized γ -lactam-based analogues was evaluated for HDAC inhibition and in cancer cell growth inhibition assays. The HDAC Fluorescent Activity Assay kit²¹ and SRB assay were used on six human cancer cell lines: PC-3 (prostate), MDA-MB-231 (breast), ACHN (renal), HCT-15 (colon), NCI-H23 (nonsmall lung), and NUGC-3 (gastric) (Table 1). The γ -lactam inhibitors showed promising HDAC

Table 1. Inhibition of HDAC Enzyme Activity and Cancer Cell Growth by γ -Lactam Analogues

compd	IC ₅₀ ^a (μ M)	GI ₅₀ ^a (μ M)					
		HDAC	PC-3	MDA-MB-231	ACHN	HCT-15	NCI-H23
SAHA	0.11	2.69	2.00	4.22	2.49	2.34	2.94
8d	0.06	5.31	1.94	5.99	4.07	4.67	6.06
8f	0.11	2.94	0.6	0.41	1.65	3.46	NT
8i	0.1	1.83	0.69	0.86	0.57	0.42	0.72
8l	0.16	7.92	3.6	7.75	>10	4.08	4.12
8m	0.15	>10	5.38	>10	>10	2.32	>10
8n	1.08	8.69	3.18	5.7	>10	4.39	6.57
8o	1.47	>10	4.97	8.96	>10	7.8	>10
Average							
8a–m	0.19	4.62	1.99	3.33	4.72	2.50	4.28
8n–v	0.42	4.14	2.76	3.60	4.25	2.55	3.38
8w–d'	0.42	3.48	2.21	3.33	5.10	2.52	2.20
8e'–f'	0.44	6.09	4.15	3.73	8.54	6.25	3.53
all	0.34	4.40	2.50	3.45	5.13	2.96	3.44

^aValues are the means of a minimum of three independent experiments. NT: not tested.

inhibitory activity, exhibiting a range of IC_{50} values from 0.04–1.47 μM . Most of these analogues also showed good cancer cell growth inhibitory activities ($GI_{50} = 0.22\text{--}10\ \mu\text{M}$). Of the six cancer cell lines, MDA-MB-231 was the most sensitive (average $GI_{50} = 2.50\ \mu\text{M}$) to the γ -lactam inhibitors, whereas HCT-15 was the least sensitive (average $GI_{50} = 5.13\ \mu\text{M}$). The structure–activity relationship revealed that the length of the carbon chain between the γ -lactam core and hydroxamate affected the HDAC inhibitory activity and cancer cell growth inhibition. In general, compounds with the two-carbon linker were more active than the other compounds (**8a–m**, **8w–f'**). With the exception of the weak activity of **8n–o** with electron withdrawing group (NO_2), the average IC_{50} value of compounds with the two-carbon linker (**8p–v**) was 0.17 μM . The two-carbon linker provides a proper fit into the active site, leading to better HDAC inhibition profiles.¹⁷ The functional groups on the cap group also affected HDAC inhibitory activity and metabolic stability. The substituents of the cap group conferred resistance to oxidation of the hydrophobic cap group by blocking the NIH shift. The substituents on the meta- and para- position (**8b** and **8c**) had better HDAC inhibitory activity than the ortho- position (**8a**). In addition, bulky and hydrophobic cap groups induced better HDAC inhibitory activity. Of the analogues synthesized, those with a nitro (**8n–o**) substituent attached on the cap group exhibited weak activity against HDAC and on cancer cell growth inhibition, whereas those with a cyano (**8l–m**) group had strong HDAC inhibitory activity but weak activity for cancer cell growth inhibition. It appears that the lone pair electrons located on the cyano group substituent may have an adverse effect on cancer cell growth inhibition activity.

Physicochemical properties have an effect on metabolic stability, which is an important factor in predicting absorption, distribution, metabolism, and excretion (ADME) profiles. The number of rotatable bonds, topological polar surface area (tPSA), and $\log D$ values of the γ -lactam analogues were predicted with the PreADME program²² (Table 2). As the

Table 2. Physicochemical Properties of the γ -Lactam Analogues

compd	<i>n</i>	R	rotatable bond no.	tPSA	$\log D$
8d	1	4-F	5	69.64	0.5714
8f	1	4-Br	5	69.94	1.2620
8i	1	4- <i>t</i> -Bu	5	69.64	2.0950
8k	1	4-bi- CF_3	5	69.64	2.3962
8l	1	3-CN	6	93.43	0.2357
8m	1	4-CN	6	93.43	0.1968
8n	2	3- NO_2	6	115.46	0.6331
8o	2	4- NO_2	6	115.46	0.5942
8v	2	4- <i>t</i> -Bu	6	69.64	2.2477
8d'	3	4- <i>t</i> -Bu	7	69.64	2.7017
8f'	4	4-Cl	8	69.64	2.1665

carbon chain length increased, the number of rotatable bonds and the lipophilicity increased. Most of the analogues had a similar tPSA of 69.64, but the cyano and nitro analogues (**8l–o**) had a large tPSA of 93.43 and 115.46, respectively. Larger tPSA values probably have relatively smaller effects on cancer cell growth inhibition due to the poor membrane permeability. The higher lipophilicity of the analogues causes metabolic instability in mouse liver microsomes, which leads to poor ADME profiles.⁴ We selected some compounds with a range of

$\log D$ values and number of rotational bonds to confirm these observations. We also evaluated their ADME profiles with microsomal stability assays and pharmacokinetic studies. Four analogues, **8d**, **8f**, **8i**, and **8k**, had one-carbon chain linkers, a small rotatable bond number (5), and the same tPSA (69.64) in common but had a wide range of lipophilicity. The other three analogues, **8v**, **8d'**, and **8f'**, had the same tPSA (69.64), similar $\log D$ values, and from one to four carbon chain linkers. These also showed good inhibitory activity against HDAC and cancer cell growth.

The positive results of the parallel artificial membrane permeability assay (PAMPA) experiment indicated that most of these compounds have a good absorption rate (Table 3). An

Table 3. PAMPA Permeability and Metabolic Stability of γ -Lactam HDAC Inhibitors

compd	PAMPA ^a		% remaining at 30 min ^d	
	P_e^b (nm/s)	R^c (%)	–NADPH	+NADPH
8d	19.31 ± 9.46	24.28	91.4	87.7
8f	10.16 ± 1.42	22.47	100.0	84
8i	21.95 ± 3.70	21.77	79.0	58.2
8k	28.32 ± 3.84	21.23	40.55	35.71
8v	65.29 ± 26.07	20.15	51.01	38.06
8d'	15.04 ± 11.96	25.35	57.63	35.32
8f'	4.94 ± 0.98	28.11	34.65	24.94
negative control	15.06 ± 0.29 ^e	18.27	96.2 ^g	100.8 ^h
positive control	63.62 ± 4.05 ^f	12.13	86.8 ^h	1.2 ^h

^aThe final concentration was 200 μM . ^bPassive diffusion. ^cMass retention. ^dMicrosomal stability was determined by incubating 1 μM of the test compounds with female ICR mouse liver microsomes (0.5 mg protein/mL) for 30 min at 37 °C. ^eRanitidine. ^fMetoprolol. ^gAtenolol. ^hChlorpromazine.

increase of lipophilicity generally leads to an increase in membrane permeability. However, compounds **8d'** and **8f'**, which have long carbon chain linkers ($n = 3$ and 4, respectively) and high $\log D$ values (2.71 and 2.16, respectively), showed low permeability. It appears that too high a lipophilicity leads to adhesion between the compounds and membrane. Metabolic stability using mouse liver microsomes showed that lipophilicity is related to metabolic stability. Highly lipophilic compounds such as **8i**, **8k**, and **8f'** were easily degraded in the mouse liver microsome with or without NADPH, whereas **8d** and **8f**, with low lipophilicity, showed good metabolic stability (Table 3). This is mainly caused by the hydrolysis and glucuronidation of the hydroxamic acid.¹⁴ On the basis of these results, low lipophilic compounds are more stable in liver microsomes but less active in HDAC inhibition than high lipophilic compounds.

The in vivo pharmacokinetic studies showed that lipophilicity and microsomal stability influence pharmacokinetic profiles (Table 4). The low metabolic stability of **8i** resulted in low oral exposure (738.6 h-ng/mL) and oral bioavailability (10.7%). However, the low lipophilic compounds **8d** and **8f** had similar C_{max} values (2302 and 2707.5 ng/mL, respectively) after oral administration, but **8f** was about three times higher than **8d** for oral exposure (3108.0 h-ng/mL compared to 1178.9 h-ng/mL). The low lipophilicity of **8d** lowered its cellular membrane permeability (caco-2 cell 7.8×10^6 cm/s) and led to low oral exposure. Overall, compound **8f** had the best oral bioavailability (44.6%) and other PK characteristics.

In conclusion, most of the synthetic γ -lactam-based HDAC inhibitors were designed to improve metabolic stability. The γ -

Table 4. Pharmacokinetic Profiles of 8d, 8f, and 8i in Balb/c Mouse

parameters ^a	unit	8d		8f		8i	
		IV	PO	IV	PO	IV	PO
dose	mg/kg	10	30	10	30	10	20
T_{max}	h		0.25		0.15		0.25
C_{max}	ng/mL		2302		2707.5		461.7
$AUC_{0-\infty}^b$	h·ng/mL	1284.9	1178.9	2325.2	3108.0	3440.3	738.6
CL	L/h/kg	7.8		4.3		2.9	
V_{ss}	L/kg	1.8		4.1		1.6	
$t_{1/2}$	h	2.6	1.1	2.8	3.1	7.8	13.6
F	%		30.6		44.6		10.7

^aPK parameters were based on the mean plasma concentration–time profiles of three animals per time point. PK parameters were calculated by noncompartmental analysis using PK Solutions 2.0 (Summit Research Services, Montrose, CO, USA). ^bAUC after iv administration was calculated from 0 to infinity, whereas the oral AUC was calculated from 0 to 5 h.

lactam core was introduced to reduce lipophilicity; the smaller core provides better inhibition profiles by fitting in the narrow binding pocket of HDAC. The diverse substituents on the cap group were also introduced to block the NIH shift and improve their microsomal stability. These HDAC inhibitors showed good in vitro antitumor activities. The analogues with a one-carbon linker between the γ -lactam core and cap group were selected for their improved microsomal stability to reduce their lipophilicity and number of rotatable bonds. Too low a lipophilicity led to poor cell permeability and oral absorption. Metabolic blockers on the bulky and hydrophobic cap group are also an important parameter for metabolic stability. Compound 8f shows both promising HDAC inhibitory activity and good PK characteristics.

EXPERIMENTAL SECTION

General Procedure for the Synthesis of 6–8. All chemicals, anhydrous solvents, and other solvents were purchased from commercial suppliers. The purity of final compounds, determined by Agilent analytic column eclipse-XDB-C18 (250 mm \times 4.6 mm, 5 μ m, or 150 mm \times 4.6 mm, 5 μ m) at a flow rate of 0.3 mL/min on Shimadzu HPLC 2010 instruments using an isocratic elution of 90% CH₃CN/H₂O 0.1% formic acid or a gradient elution of 20–80% CH₃CN in 0.1% aqueous formic acid over 30 min, was found to be >95%.

4-[Allyl-(4-bromo-benzyl)-carbomoyl]-pent-4-enoic Acid Methyl Ester (6f). A mixture of 4f (400 mg, 1.77 mmol), monoacid (5, 460 mg, 2.12 mmol), EDC (602 mg, 2.30 mmol), and DMAP (89 mg, 0.53 mmol) in anhydrous dichloromethane (5 mL) was stirred at room temperature for 12 h under Ar atmosphere. The mixture was quenched by 10% HCl (aq) at pH 1 and extracted with dichloromethane (10 mL \times 2). The organic phase was washed with sodium bicarbonate (aq) and brine, dried over sodium sulfate, and then filtered and concentrated in vacuo to yield the crude product, which was purified by column chromatography (silica gel, 1:2 ethyl acetate/hexane), yielding 6f as a colorless oil (430 mg, 69%). ¹H NMR (300 MHz, CDCl₃) δ 7.33–7.17 (m, 4H), 5.68 (br s, 1H), 5.10–4.98 (m, 4H), 3.62 (s, 3H), 3.37 (s, 2H), 2.57 (dd, 4H, J_A = 8.3 Hz, J_B = 5.4 Hz), 2.26 (s, 2H).

3-[1-(4-Bromo-benzyl)-2-oxo-2,5-dihydro-1H-pyrrol-3-yl]-propionic Acid Methyl Ester (7f). A mixture of 6f (400 mg, 1.2 mmol) and 2nd generation Grubbs' catalyst (108 mg, 0.12 mmol) in anhydrous dichloromethane (136 mL) was stirred at reflux for 12 h under an Ar atmosphere in the dark. The mixture was concentrated in vacuo to yield the crude product, which was purified by column chromatography (silica gel, 1:1 ethyl acetate/hexane), yielding 7f as a dark-gray oil (100 mg, 27%). ¹H NMR (300 MHz, CDCl₃) δ 7.29 (d, 2H, J = 8.4 Hz), 6.97 (d, 2H, J = 8.1 Hz), 6.57 (s, 1H), 4.43 (s, 2H), 3.62 (s, 3H), 3.53 (s, 2H), 2.50 (s, 2H), 2.45 (s, 2H).

3-[1-(4-Bromo-benzyl)-2-oxo-2,5-dihydro-1H-pyrrol-3-yl]-N-hydroxy-propionamide (8f). A mixture of 7f (100 mg, 0.30 mmol) and

1.7 M KONH₂ (0.9 mL, 1.50 mmol) in anhydrous methanol (3.0 mL) was stirred at 0 °C for 12 h. The mixture was concentrated in vacuo to yield the crude product, which was purified by column chromatography (silica gel, 5% methanol in dichloromethane), yielding 8f as an orange solid (20 mg, 20%). ¹H NMR (500 MHz, DMSO-*d*₆) 10.43 (s, 1H), 8.71 (s, 1H), 7.52 (d, 2H, J = 8.5 Hz), 7.14 (d, 2H, J = 8.5 Hz), 6.83 (s, 1H), 4.51 (s, 2H), 3.80 (s, 2H), 2.40 (t, 2H, J = 6.7 Hz), 2.21 (t, 2H, J = 7.5 Hz). ¹³C NMR (125 MHz, DMSO-*d*₆) δ 171.17, 168.89, 138.08, 137.89, 137.28, 132.17, 130.45, 120.98, 50.96, 45.35, 30.79, 22.20. ESI (*m/z*) 339, 341 (MH⁺), 361, 363 (MNa⁺). HRMS (FAB⁺) calcd for C₁₄H₁₅BrN₂O₃ (MH⁺) 339.0344, found 339.0345. HPLC (t_R : purity = 9.52 min, 98.55%).

ASSOCIATED CONTENT

Supporting Information

Detailed information on the biological data, analytical data, and the HPLC method for final compound 8 and recommended compound characterization checklist (XLS). This material is available free of charge via the Internet at <http://pubs.acs.org>.

AUTHOR INFORMATION

Corresponding Author

*Phone: +82 2 2123 2882. Fax: +82 2 362 7265. E-mail: gyoonhee@yonsei.ac.kr.

Author Contributions

These authors contributed equally to this work.

Notes

The authors declare no competing financial interest.

ACKNOWLEDGMENTS

This research was supported by National Research Foundation (2012-0000884), Korea Research WCU grant (R31-2008-000-10086-0), and Brain Korea 21 project, Republic of Korea.

ABBREVIATIONS USED

HDAC, histone deacetylase; HAT, histone acetyltransferase; QSAR, quantitative structure–activity relationship; tPSA, topological polar surface area; EDC, *N*-(3-dimethylaminopropyl)-*N'*-ethylcarbodiimide hydrochloride; DMAP, 4-(*N,N*-dimethylamino)pyridine; PK, pharmacokinetics; ADME, absorption, distribution, metabolism, and excretion

REFERENCES

- (1) Lemoine, M.; Younes, A. Histone deacetylase inhibitors in the treatment of lymphoma. *Discovery Med.* **2010**, *10*, 462–470.
- (2) Carafa, V.; Nebbioso, A.; Altucci, L. Histone deacetylase inhibitors: recent insights from basic to clinical knowledge and

patenting of anti-cancer actions. *Recent Pat. Anti-Cancer Drug Discovery* **2011**, *6*, 131–145.

(3) Kang, M. R.; Kang, J. S.; Han, S. B.; Kim, J. H.; Kim, D. M.; Lee, K.; Lee, C. W.; Lee, K. H.; Lee, C. H.; Han, G.; Kim, H. M.; Park, S. K. A novel delta-lactam-based histone deacetylase inhibitor, KBH-A42, induces cell cycle arrest and apoptosis in colon cancer cells. *Biochem. Pharmacol.* **2009**, *78*, 486–194.

(4) Yoon, H. C.; Choi, E.; Park, J. E.; Cho, M.; Seo, J. J.; Oh, S. J.; Kang, J. S.; Kim, H. M.; Park, S. K.; Lee, K.; Han, G. Property based optimization of delta-lactam HDAC inhibitors for metabolic stability. *Bioorg. Med. Chem. Lett.* **2010**, *20*, 6808–6811.

(5) Kim, H. M.; Lee, K.; Park, B. W.; Ryu, D. K.; Kim, K.; Lee, C. W.; Park, S. K.; Han, J. W.; Lee, H. Y.; Han, G. Synthesis, enzymatic inhibition, and cancer cell growth inhibition of novel delta-lactam-based histone deacetylase (HDAC) inhibitors. *Bioorg. Med. Chem. Lett.* **2006**, *16*, 4068–4070.

(6) Mai, A.; Massa, S.; Rotili, D.; Cerbara, I.; Valente, S.; Pezzi, R.; Simeoni, S.; Ragno, R. Histone deacetylation in epigenetics: an attractive target for anticancer therapy. *Med. Res. Rev.* **2005**, *25*, 261–309.

(7) Muri, E. M. F.; Nieto, M. J.; Sindelar, R. D.; Williamson, J. S. Hydroxamic acids as pharmacological agents. *Curr. Med. Chem.* **2002**, *9*, 1631–1653.

(8) Kavanaugh, S. M.; White, L. A.; Kolesar, J. M. Vorinostat: a novel therapy for the treatment of cutaneous T-cell lymphoma. *Am. J. Health-Syst. Pharm.* **2010**, *67*, 793–797.

(9) Vigushin, D. M.; Ali, S.; Pace, P. E.; Mirsaidi, N.; Ito, K.; Adcock, I.; Coombes, R. C. Trichostatin A is a histone deacetylase inhibitor with potent antitumor activity against breast cancer in vivo. *Clin. Cancer Res.* **2001**, *7*, 971–976.

(10) Vassiliou, S.; Mucha, A.; Cuniassé, P.; Georgiadis, D.; Lucet-Levannier, K.; Beau, F.; Kannan, R.; Murphy, G.; Knauper, V.; Rio, M. C.; Basset, P.; Yiotakis, A.; Dive, V. Phosphinic pseudo-tripeptides as potent inhibitors of matrix metalloproteinases: a structure–activity study. *J. Med. Chem.* **1999**, *42*, 2610–2620.

(11) Whittaker, M.; Floyd, C. D.; Brown, P.; Gearing, A. J. Design and therapeutic application of matrix metalloproteinase inhibitors. *Chem. Rev.* **1999**, *99*, 2735–2776.

(12) Choi, E.; Lee, C.; Park, J. E.; Seo, J. J.; Cho, M.; Kang, J. S.; Kim, H. M.; Park, S. K.; Lee, K.; Han, G. Structure and property based design, synthesis and biological evaluation of gamma-lactam based HDAC inhibitors. *Bioorg. Med. Chem. Lett.* **2011**, *21*, 1218–1221.

(13) Kwon, H. K.; Ahn, S. H.; Park, S. H.; Park, J. H.; Park, J. W.; Kim, H. M.; Park, S. K.; Lee, K.; Lee, C. W.; Choi, E.; Han, G.; Han, J. W. A novel gamma-lactam-based histone deacetylase inhibitor potently inhibits the growth of human breast and renal cancer cells. *Biol. Pharm. Bull.* **2009**, *32*, 1723–1727.

(14) Kim, H. M.; Oh, S. J.; Park, S. K.; Han, G.; Kim, K.; Lee, K. S.; Kang, J. S.; Nam, M.; Lee, K. In vitro metabolism of KBH-A40, a novel delta-lactam-based histone deacetylase (HDAC) inhibitor, in human liver microsomes and serum. *Xenobiotica* **2008**, *38*, 281–293.

(15) Kim, H. M.; Ryu, D. K.; Choi, Y.; Park, B. W.; Lee, K.; Han, S. B.; Lee, C. W.; Kang, M. R.; Kang, J. S.; Boovanahalli, S. K.; Park, S. K.; Han, J. W.; Chun, T. G.; Lee, H. Y.; Nam, K. Y.; Choi, E. H.; Han, G. Structure–activity relationship studies of a series of novel delta-lactam-based histone deacetylase inhibitors. *J. Med. Chem.* **2007**, *50*, 2737–2741.

(16) Kim, H. M.; Hong, S. H.; Kim, M. S.; Lee, C. W.; Kang, J. S.; Lee, K.; Park, S. K.; Han, J. W.; Lee, H. Y.; Choi, Y.; Kwon, H. J.; Han, G. Modification of cap group in delta-lactam-based histone deacetylase (HDAC) inhibitors. *Bioorg. Med. Chem. Lett.* **2007**, *17*, 6234–6238.

(17) Lee, C.; Choi, E.; Cho, M.; Lee, B.; Oh, S. J.; Park, S. K.; Lee, K.; Kim, H. M.; Han, G. Structure and property based design, synthesis and biological evaluation of γ -lactam based HDAC inhibitors: Part II. *Bioorg. Med. Chem. Lett.* **2012**, *22*, 4189–4192.

(18) Yang, J. S.; Chun, T. G.; Nam, K. Y.; Kim, H. M.; Han, G. Structure–Activity Relationship of Novel Lactam Based Histone Deacetylase Inhibitors as Potential Anticancer Drugs. *Bull. Korean Chem. Soc.* **2012**, *33*, 2063–2066.

(19) Bressi, J. C.; Jennings, A. J.; Skene, R.; Wu, Y.; Melkus, R.; De Jong, R.; O'Connell, S.; Grimshaw, C. E.; Navre, M.; Gangloff, A. R. Exploration of the HDAC2 foot pocket: synthesis and SAR of substituted *N*-(2-aminophenyl)benzamides. *Bioorg. Med. Chem. Lett.* **2010**, *20*, 3142–3145.

(20) *Accelrys Discovery Studio 3.0*; Accelrys Software, Inc.: San Diego, 2011.

(21) *HDAC Fluorescent Activity Assay/Drug Discovery Kit AK-500*, BIOMOL International, Inc.: Plymouth Meeting, PA.

(22) *PreADMET 2.0*; BMDRC: Seoul, 2007.